The strength of rotary-straightened steel columns

Xiaomeng Ge[1], Joseph A. Yura[2]

Abstract

A study was undertaken to determine the strength of rotary-straightened steel columns. Almost all steel sections are now rotary-straightened as standard practice. Current column design formulas are based on tests and analytical studies of unstraightened columns that contain compressive residual stress at the flange tips, typical of the manufacturing processes for most steel column sections rolled during 1950-1970. A rotary-straightened W12x65 grade 50 ksi column-type section was evaluated experimentally to determine residual stresses, out-of-straightness and material properties. The measured out-of-straightness averaged L/ 1400 in the weak direction and L/ 9500 in the strong direction. The residual stresses in the flanges were primarily tensile with the value at the tips exceeding 10 ksi. Analytical column curves were developed using residual stresses and out-of-straightness for measured values and typical values used in previous studies. The result showed that weak axis column strength was improved up to 25%, using the rotarized residual stress pattern, compared to the compressive residual stress pattern typically used. For weak axis stability, the rotarized residual stress pattern gave 6% higher column strength compared to neglecting residual stress. For strong axis behavior, the effect of rotarized residual stress was only 1% compared to neglecting residual stress. Analytical studies on some sample unbraced frames showed that weak axis frame strength improved up to 60% with the rotary-straightened stress pattern compared to frames with $0.3F_y$ compressive residual stresses. Neglecting residual stresses provided up to 45% increase in strength. This implies that it would be conservative to neglect residual stress when evaluating frame and beam-column behavior for W-shapes and inelasticity has a diminishing effect.

1. Introduction

1.1 Background

Current column formulas are based on the ultimate strength of axially-loaded compression members that have initial out-of-straightness and compressive residual stresses at the flange tips. While initial out-of-straightness has been considered in evaluating column strength since the mid-1800's (Ayton, Perry 1886), the effect of compressive residual stress on column strength has been a more recent development (Beedle, Tall 1960). The residual stresses in rolled shapes are caused by differential cooling of the cross section in air after rolling; the tips of the flanges cool

---

[1] Graduate Research Assistant, University of Texas at Austin, < xmge@utexas.edu>
[2] Emeritus Professor, University of Texas at Austin, <yura@mail.utexas.edu>

first resulting in compressive stresses and tensile stresses develop at the flange-web junction, the last location to cool. Welding also causes residual stresses but such sections are beyond the scope of this research. Figure 1, adapted from Beedle, Tall 1960, shows a common measured pattern of residual stresses. In analytical column studies it is usually assumed that the value of the compressive residual stress at the flange tips, F_{rc}, is 0.3 F_y where F_y is the yield strength of the section, even though it is well known that cooling residual stresses are not affected by the value of F_y. Since most of the measured residual stress data were obtained from 36 ksi steel during the 1950-75 time period, $F_{rc} = 0.3 \times 36 = 10.8$ ksi would be more appropriate for use with higher steel strengths. During this time period many rolled sections were gag-straightened (weak axis loading to plastify the flanges at discrete points along the length) while small sections were continuously plastified (rotarized) in a machine with a series of rollers as shown in Fig. 2.
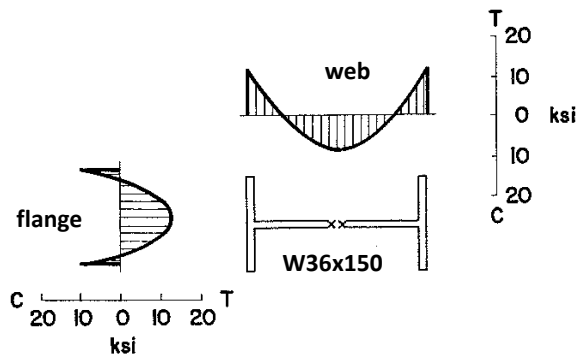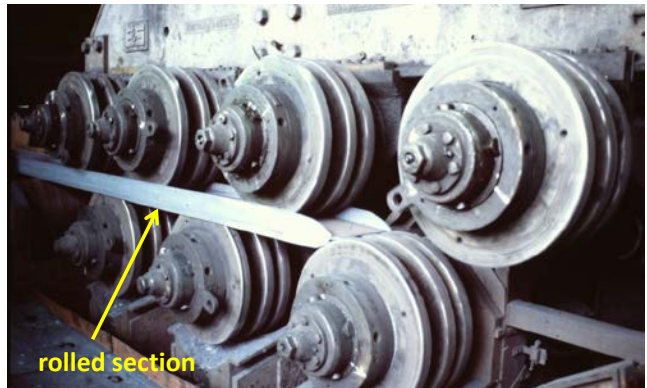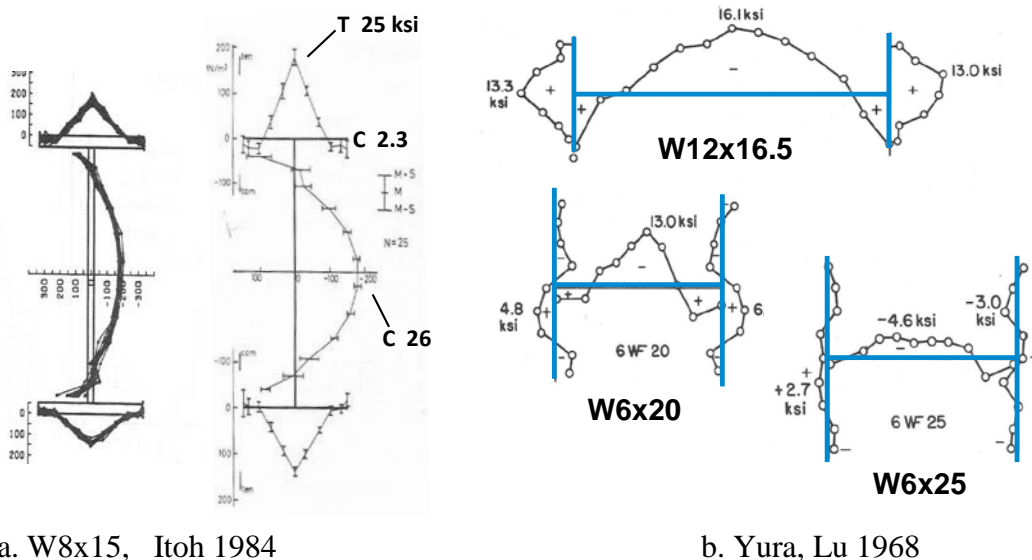

Figure 1: Residual Stress Pattern

Figure 2: Rotary-Straightening

Rotary-straightening alters the cooling residual stress pattern in the flanges as shown by the measured patterns in Fig. 3 for small members in the U.S. and Japan. In general the rotarizing process removes or greatly reduces the compressive residual stresses at the flange tips. The results in Fig. 3a are from samples taken from twenty-five, 23 ft long, W8x15 members. There is

a. W8x15, Itoh 1984

b. Yura, Lu 1968

Figure 3: Rotary- Straightened Residual Stresses

little scatter and the results shown are consistent with those reported by researchers in Great Britain, Australia and Canada. Since compressive residual stresses at the flange tips significantly reduce weak-axis column strength in the mid-slenderness ratio range, their reduction or removable can have economic benefits. Alpsten (1972) studied the effect of rotary straightening on column strength theoretically and with column tests; his research is summarized in ECCS (1976). From this 1976 summary,

> "From the column investigations it may be concluded that the beneficial effects of a roller-straightening procedure are reliable. The increase in column strength due to roller straightening is of the order of 10 to 20 percent in the most interesting range of slenderness ratio (L/r ~ 40 to 100), and may for a suitable roller-straightening procedure be well over 20 percent"

> "Since most, if not all, small to medium-size hot-rolled members are indeed roller-straightened in modern steel mills, it appears that the above is of considerable economical significance. Recognizing the beneficial effect of the roller-straightening in the design procedure for columns will also serve as a stimulus to the producers towards a more general application of roller-straightening in the rolling mills, that is, also for large and deep cross sections."

Compression member design procedures in 1970 did not take advantage of rotary-straightening benefits mainly because the process and equipment available at that time limited the number of sections that could be rotarized. But the steel manufacturing and rolling practices have improved considerably since 1980. Continuous casting into the dog-bone shape and continuous rolling have greatly improved the efficiency in steel shape production. Improved equipment and procedures currently permit rotary-straightening of sections that weigh almost 400 lb/ft and depths to 36 in. so most sections are now rotarized. It appears that the benefits of rotary straightening should be reevaluated for developing design procedures for rolled compression members based on the current manufacturing methods.

1.2 Research Plan
A pilot experimental and analytical research program was developed to investigate the variables that affect column and frame strength with a column larger than the W8x31 that has been used extensively in studies related to current design methods. A W12x65 section was chosen for this program. Material properties, geometric imperfections and residual stresses were measured. These experimental data are reported in Section 2. Guided by the measured data, column curves were derived using finite element inelastic 2nd order analysis and compared with solutions using traditional out-of-straightness and compressive flange-tip residual stresses in Section3. The load-deflection responses of a few unbraced frames were also analyzed and potential practical design approaches are discussed in Section 4.

2. Experimental studies

2.1 Geometric out-of-straightness
Out-of-straightnesses of five 40 ft. long W12X65 sections were measured in the strong direction, with three of the lengths in the weak direction, as well. The strong and the weak axis initial out-of-straightness are identified as camber and sweep respectively. For the measurement of camber in the strong direction, each section was simply supported at both ends with the web vertical, and the vertical displacement between the center of the top flange and a steel wire, which was pre-tensioned by a heavy object to maintain the straightness at a constant level, was measured by a

digital spiral micrometer every two feet. To eliminate the self-weight deformation of both the steel section and steel wire, the measurement procedure was repeated after flipping over the section. Half of the difference between these two measurements is the initial camber at the specific location. For the measurement of the initial sweep in the weak direction, each member was oriented with the web vertical. A pre-tensioned steel wire was suspended next to one of the top flange tips. The horizontal distance between the flange tip and steel wire was measured every two feet. Then, the section was flipped over to measure the sweep in the other flange. The average of these two measurement values is defined as the initial sweep in the weak direction, and the difference between these two values when divided by the nominal depth of 12 in. defines the initial twist along the section.

The data for initial camber, sweep, and twist are shown in Figs. 4(a), (b), and (c) respectively. As shown in Fig. 4(a), the strong axis out-of-straightness was between 1/26300 and 1/ 3850 over the measurement length of 36 ft. All these length are very straight relative to the L/1000 value assumed in analytical column studies. Three of the members had a significantly larger camber profile than the other two members. This was due to an obvious kink of unknown origin located somewhere within the 40 ft. length. If the maximum camber section (green line) is divided into two 18 ft long members, the initial camber of each half will decrease to 1/8100 and 1/12200 of the 18 ft. length compared to 1/3850 for the 40 ft length. In general shorter lengths will have smaller initial out-of-straightness. The average maximum camber for the five lengths is 1/9600.
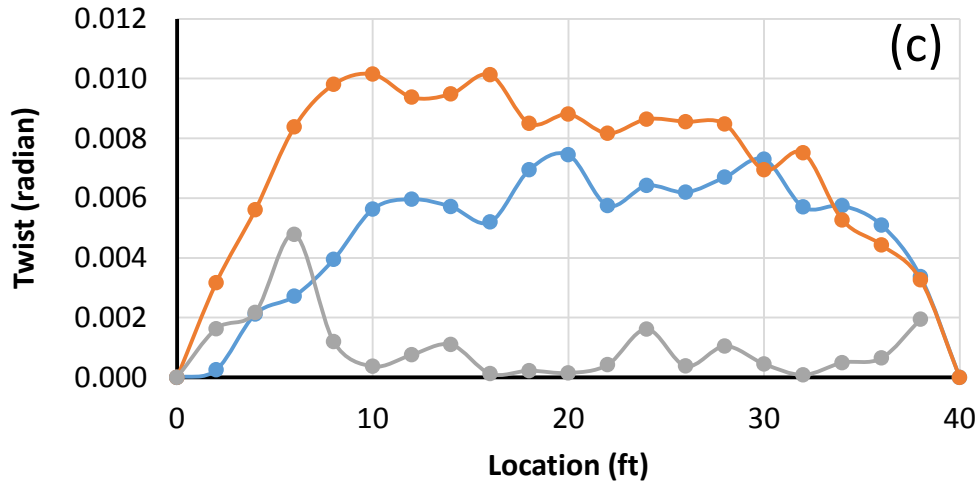

4
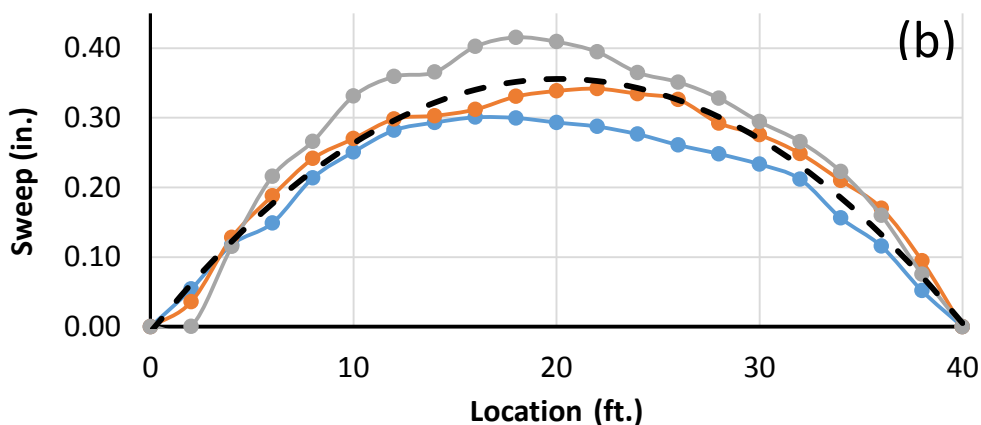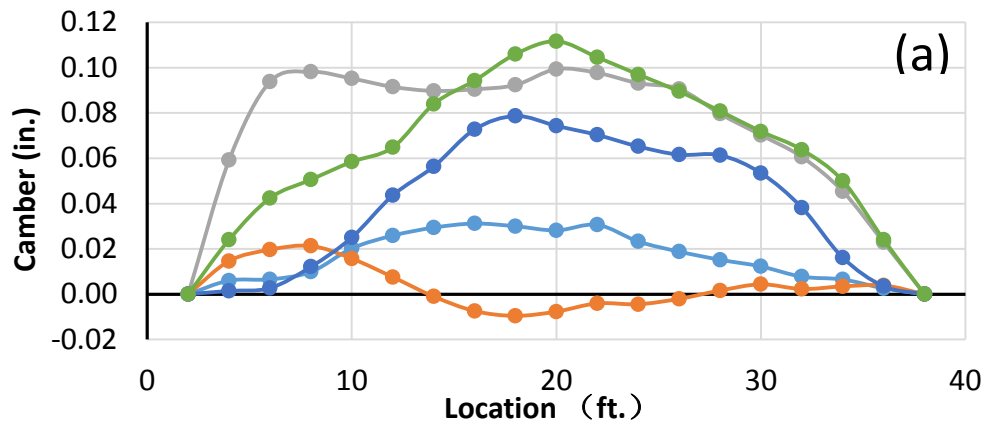
Figure 4: W12X65 Geometric Imperfections, (a) Camber, (b) Sweep (c) Twist

The average sweep in the weak direction from all three members is approximately 1/1400 of the section length, whose profile could be well fitted by a circle function with a radius averaged at 6700 ft, as shown dashed in the Fig. 4(b). If two 20 ft members ($L/r_y = 80$) are cut from the 40 ft length, the average weak-axis out-of-straightness would be 1/2700. The twist along the length of all three sections had a max value no larger than 0.011radians (0.6°). The maximum measured twist value corresponds to a 0.132 in. relative lateral displacement between the two flanges, which is 1/3600 of the total length, smaller than the assumed initial twist value of 1/1000 in the torsional bracing provisions of the 2010 AISC Specification. All geometric imperfections were smaller than those assumed in the development of stability design provisions.

2.2 Residual stress measurement
The sectioning method in *Technical Memorandum No. 6: Determination of Residual Stresses* (SSRC 2010), based on the principle that internal stresses are relieved by cutting the cross section into many small strips, was used to determine the residual stress distribution in one cross section. A 5 ft. long portion was selected and saw cut from one 40 ft. long W12x65 member. The middle 17 in. of this length would be cut strip by strip to determine the residual stresses on this cross section. The strip width at both flanges and the web was 0.75 in, while the cross-section was divided into 14 strips on each flange, 12 strips on the web and two irregular-shape strips at the flange-web junction. Small predrilled stainless steel disks were epoxied a nominal 400mm (15.75 in.) apart to the surface of the W12x65 on both sides of the flanges and the web. Initial distances between the disks were measured using a 400 mm DEMEC mechanical strain gage as shown in Fig 5. The measurement accuracy of the gauge is four microstrain (0.12 ksi for steel). After the initial readings were recorded, this selected portion was separated into total 42 strips by cutting with a lubricate-cooled vertical band-saw. The length of each strip on both sides was measured again after any residual stress was relieved and the deformations on both sides were averaged to eliminate the effect of any bending curvature. However, in three strips a measurement disk fell off during the slicing process so an alternative method (Yang et al 2016) was used for those strips to determine the average residual stress. A strip was clamped to a flat milling machine table to eliminate strip curvature and the average deformation was measured directly from data on one side, as shown in Fig. 6.

5
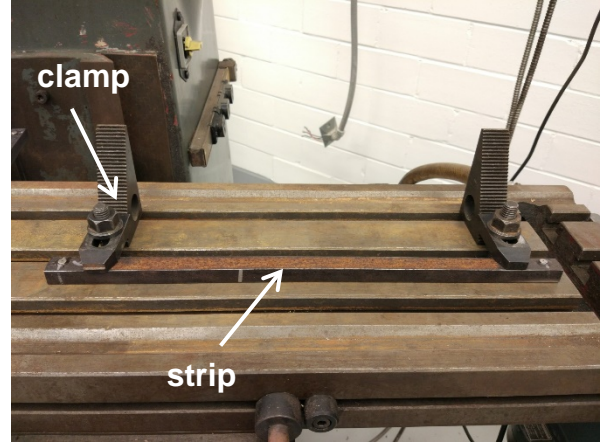
Figure 5: Initial Measurement

Figure 6: Alternative Measurement Method

The pre-averaged measured residual stress distribution is shown in Fig. 7(a). The bending effect is significant at the flange tips and near the flange-web junctions probably due to rotary-straightening. The averaged residual stress distribution in the measured cross section is shown by the solid black lines in Fig. 7(b). The disequilibrium stress for the whole section is 0.6 ksi in tension. The maximum compression stress is -12.4 ksi at the middle of the web, while the maximum tensile stress is 14.5 ksi at one flange tip. The current data is compared to the residual stresses on a W12x65 unstraightened member from Gozum (1955) by the dashed lines adapted from (Tebedge, Tall, 1974). The maximum web residual stresses are similar but the flange stresses are quite different, especially at the tips, which average at 10.9 ksi tension for the rotarized section but 20 ksi in compression for the unstraightened section.
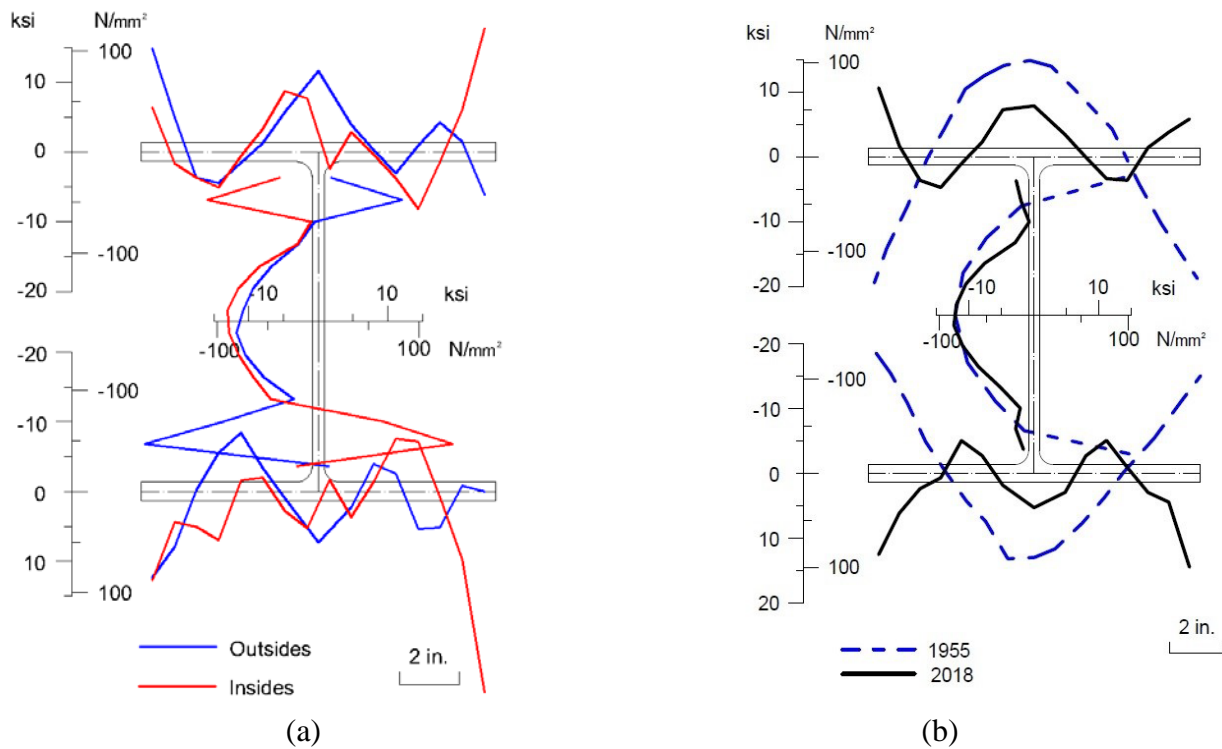

(a)

(b)

Figure 7: Residual Stress Distribution

6

2.3 Material Properties

Six coupons were sampled (ASTM 2016) at one cross section near the selected portion for residual stress measurement; two from the flange tips, two from the flanges near flange-web junctions, one from the web near one flange-web junction, and the last one was from the middle of the web as shown in Fig. 8(a). Static yield stress, dynamic yield stress, and ultimate elongation were determined using a 440 kip MTS machine and instrumented with a 200 mm extensometer. The stress-strain profile is shown in Fig. 8(b) and numerical results summarized in Table 1. For all these six samples, the static yield stress is higher than the 50 ksi required by ASTM A992 standard (2015) and is approximately 2 ksi lower than the dynamic yield stress. The ultimate elongation ranges from 21.2% to 27.7%. The static yield stresses of the two at the tips (55.2 and 58.9 ksi) are 8% higher than the two near the flange-web junctions (52.2 and 53.0 ksi). While this might appear to indicate an effect of cold straightening, Alpsten (1972) found the same percent disparity between the yield strengths of flange tip and interior flange coupons for unstraightened members so the rotarizing does not appear to affect the yield strength.
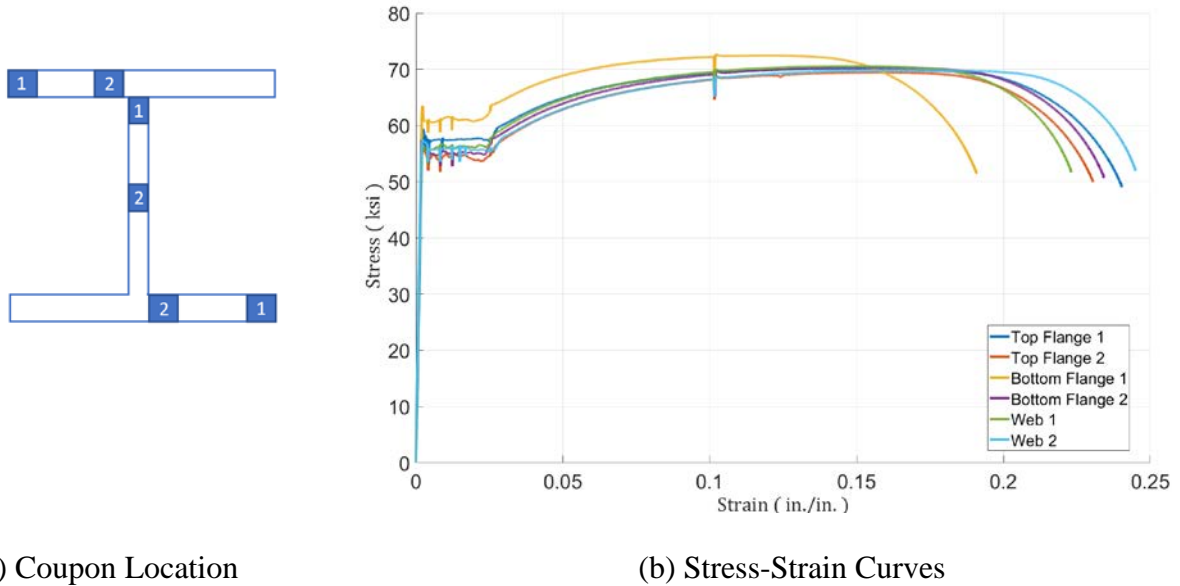

(a) Coupon Location   (b) Stress-Strain Curves

Figure 8: Steel Coupon Tension Test

Table 1: Steel Coupon Tension Test Result

Coupon	Static F_y (ksi)	Dynamic F_y (ksi)	F_u (ksi)	Elong (%)
TF1	55.2	57.6	70.1	26.7
TF2	52.2	53.9	69.5	25.9
BF1	58.9	61.1	72.7	21.2
BF2	53.0	55.3	70.3	26.3
Web1	54.9	56.2	70.5	24.7
Web2	53.7	55.7	69.9	27.2

3. Modeling
In conjunction with the experimental investigation, a series of numerical in-plane simulations was carried out to maximum load using the general-purpose finite element analysis software ABAQUS (Simulia, D. 2017) for L/r from 30 to 210 in increments of 10 L/r. The standard method was chosen for analysis, involving both material and geometry nonlinearities.

3.1 Input
The initial geometry imperfection was considered corresponding to the analyzed direction only, either the weak or strong axis direction. The geometric imperfection profile was a sine curve, the same as the first-order Euler buckling mode. Various values of maximum initial out-of-straightness were investigated, mainly L/1000. Some additional maximum midspan maximum values were based on the actual measurements documented in *Section 2.1*.

The nominal dimension of the column section was modeled without considering the fillets at the flange-web junctions, compromised by two small overlaps also located at flange-web junctions. The four-node doubly curved shell element, S4, was employed herein. With regards to the mesh size, each flange and the web was divided into six elements in the cross-section plan, and the mesh size in the longitudinal direction was half of the radius of gyration, as shown in Fig. 9.

The residual stress distribution was applied by the predefined norm stress field, which was uniform in each element but varied for the whole cross section. The classical Ketter residual stress distribution (Ketter et al 1955) and a simplified rotarized residual stress pattern, as shown in Figs. 10(a) and (b), were considered along with no residual stresses. The simplified rotarized residual stress shown by the dashed lines is the averaged and linearized model based on the measured result shown in red.

The steel material was modeled by a bilinear stress-strain curve, elastic with Young's modulus E = 29000 ksi up to F_y, followed by a plastic yield plateau until the strain = 0.20. The F_y = 36 ksi for model validation and 50 ksi for parametric study and the Poisson's ratio was 0.3.
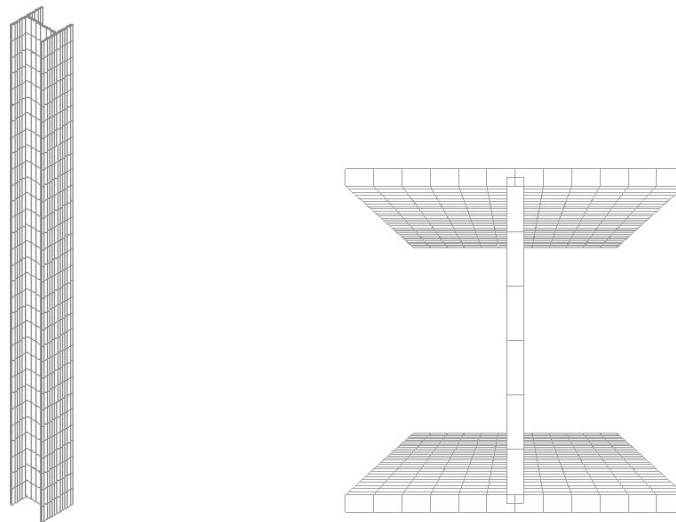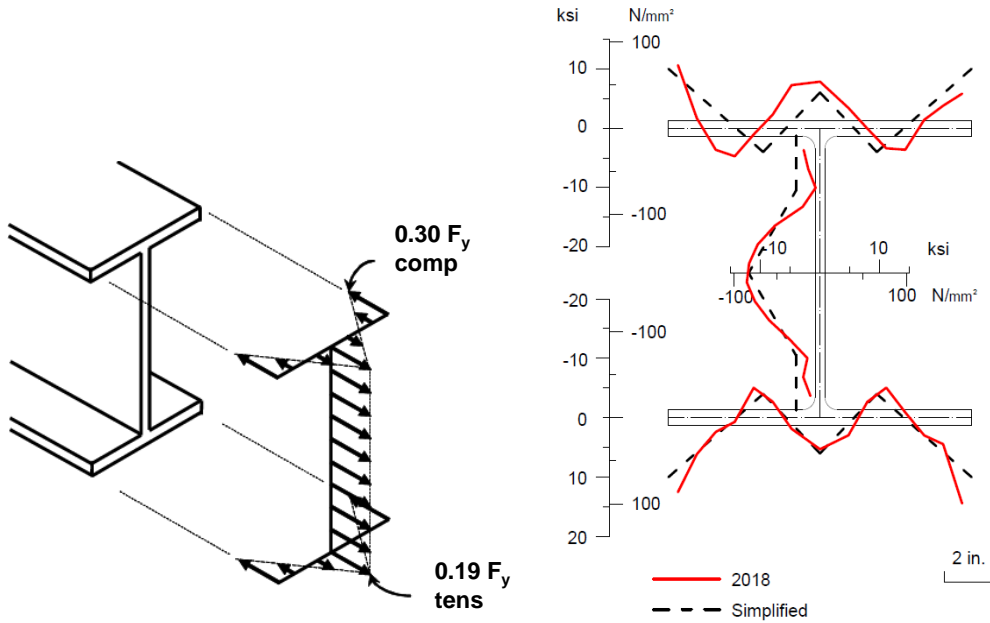

Figure 9: Finite Element Mesh

(a) Ketter Residual Stress   (b) Rotarized Pattern, Actual and Simplified

Figure 10: Residual Stress Distribution

Pinned-end boundary conditions were utilized for the analysis. For weak axis bending the displacement of the top and bottom edges of the web was restrained in the weak axis direction, as well as the movement of the bottom edges of the web in the longitudinal direction. To avoid rigid body movement, the strong-axis displacement was also restrained at the center of the web at both ends. For the model of strong axis bending, the center of the web was restrained at both ends of the column section, in both strong and weak axis direction, as well as the longitudinal direction only for the bottom. To avoid lateral-torsion buckling during strong axis bending analysis, the flange-web junctions at both ends and the middle section of the column were restrained in the weak direction. To minimize the stress concentration at each end, a uniform compression load was applied at both ends, whose direction would be constant during the monotonic loading process.

3.2 Validation of the numerical model
The numerical model was initially validated against two independent finite element models (Shen, Lu 1983; Galambos 1983) before being utilized to conduct parametric studies. A series of W8x31 columns with 36 ksi yield stress, L/1000 sine-shaped geometric imperfection at the midspan, δ_o, and Ketter residual stress distribution but with the slenderness parameter λ varied between 0.3 - 2.0 was analyzed for validation, where the slenderness parameter $\lambda = \dfrac{L}{\pi r}\sqrt{\dfrac{F_y}{E}}$. As shown in Fig. 11, the column curve for weak axis bending conducted by ABAQUS (orange dots) is similar to those obtained in 1983 within the slenderness between 0.3 and 2.0, equivalent to slender ratios *L/r* between 30 and 180. The good agreement indicates that the ABAQUS modeling approach for 2nd order inelastic analysis is reliable.
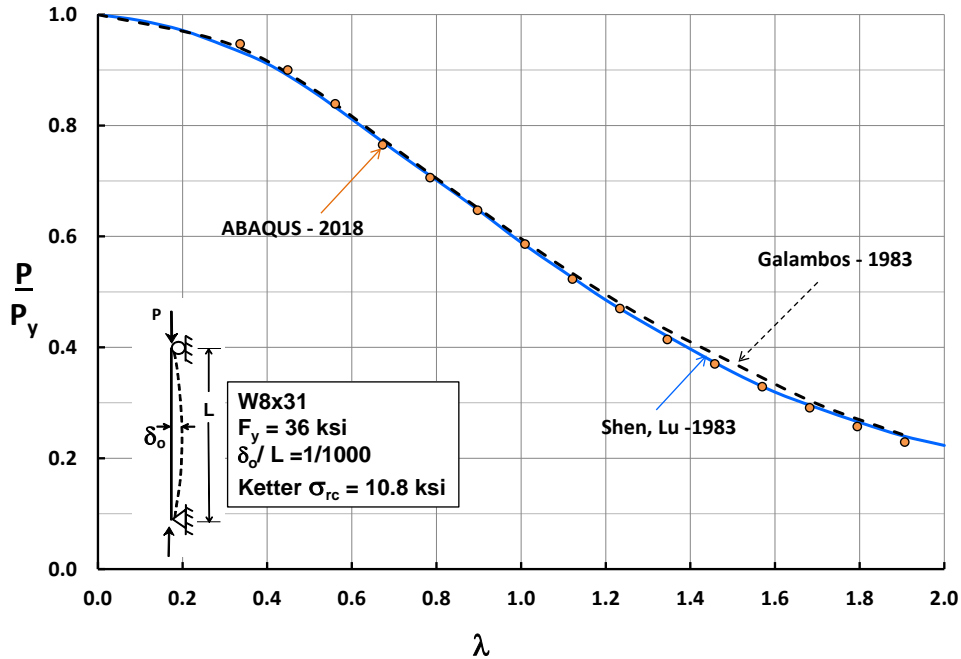
9

Figure 11: Comparison of ABAQUS Results with Other Solutions

4. Column Parametric Study

Column curves over the range of $30 < L/r < 210$ were developed for a W12x65 with $F_y = 50$ ksi using the input parameters related to residual stresses and initial out-of-straightness for both the strong and weak bending axes. No end restraint was considered. Except for one case where δ_o /L increased as the column length increased, the initial sine imperfection profile for all column lengths had a constant δ_o/L. The column curves from the study are shown in Figs. 12-15.
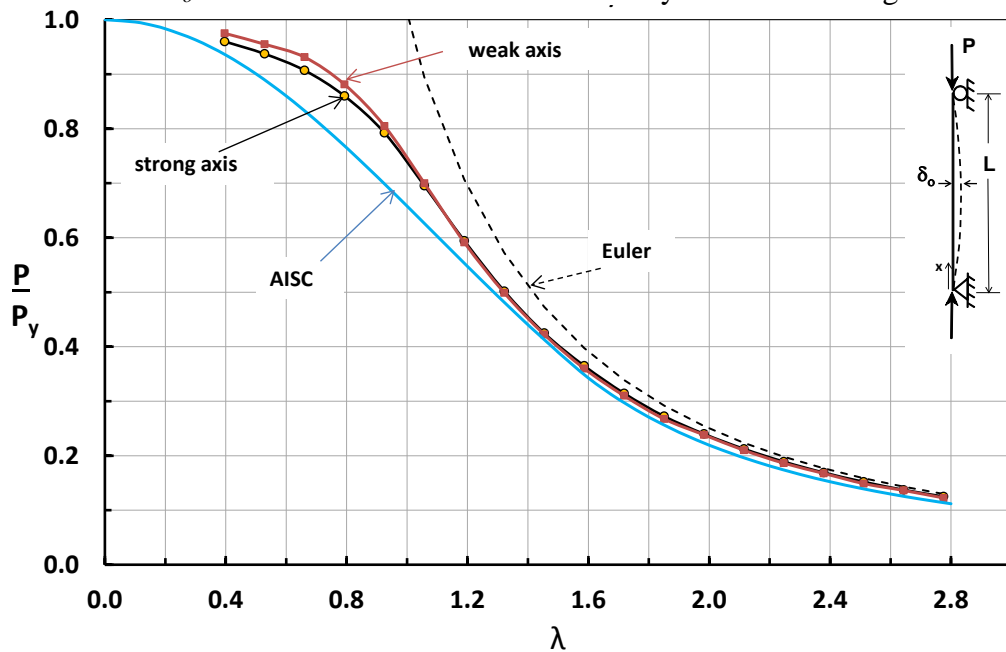

Figure 12: Column Curves- Rotarized Pattern, sine $\delta_o = L/1000$

10

Figure 12 compares the weak and strong axis ultimate column strengths based on the simplified rotary-straightened residual stress profile (Fig. 10b) and $\delta_o /L = 1/1000$. The two rotarized curves are shown with markers along with the AISC column curve and the elastic Euler solution. The rotarized solutions are close to AISC for slender columns with $\lambda > 1.2$ but significantly greater up to 15%, for shorter unbraced lengths even though the AISC solution considers some helpful small end restraint (Yura, 2018). The ratio of the weak and the strong solutions are very close to each other, within an average of 0.24% and a maximum difference of 2% at low column slenderness. Because of the favorable tension residual stress at the flange tips, the weak axis column curve is slightly greater than the strong axis which is opposite from solutions with Ketter residual stresses that have compression at the flange tips.

Figure 13 shows two plots that examine the effect of different residual stress patterns and magnitudes. Two Ketter solutions are shown for $F_y = 50$ ksi: $0.3 \ F_y = 15$ ksi and 10.8 ksi maximum compressive residual stress at the flange tips. It is well known that cooling residual stresses from rolled sections are not a function of F_y but unfortunately experimental residual-stress measurements are often non-dimensionalized by the material yield point. Most of the residual stress data on rolled sections is from the 1960 era when $F_y = 36$ ksi so the 10.8 ksi value would be the proper value to be used with higher strength streels currently in use. The AISC column curve is close to the weak-axis Ketter 10.8 ksi solution that does not consider any end restraint. The magnitude of the initial out-of-straightness is L/1000 for all the column curves in Fig. 13. The solutions for no residual stresses are close to the rotarized cases for both the strong and weak axes; for the weak axis, the no residual is on average 2% less with a maximum of 5% less and for the strong axis the statistics are 0.4% average with a 1% unconservative maximum. The no-residual weak-axis solution is on average 5% higher with maximums near 10% higher than the current AISC solution. This indicates that neglecting residual stresses for column design of rotarized sections is a viable option for developing practical design recommendations. As expected the solutions show that residual stresses have less of an effect on strong axis bending by noting the narrower band of column curves compared to the weak axis band.

The effect of δ_o /L on the weak-axis strength of columns with and without rotary straightening is shown in Fig. 14. The solutions for $\delta_o /L = 1/1000$ have been shown previously. The average measured sweep on the three 40 ft members was 1/1400 and followed a circular geometry. Maintaining that particular circular geometry but using other lengths gives a variable δ_o /L as illustrated in *Section 2.1*. For each 10 L/r increment in the weak direction a δ_o /L was calculated and used as input. The large arrows along the λ axis locate some sample δ_o /L values along the length. At $\lambda = 2.8$ that would be an approximate 50 ft long member, the out-of-straightness is 1/1000; at $\lambda = 0.8$, the 15 ft member has a $\delta_o /L = 1/3600$. Shorter members have a smaller relative out-of-straightness. The use of a variable δ_o /L gives significantly higher capacities for $\lambda < 1.3$, (L/r < 100), averaging 7% and 9% for rotarizes and Ketter conditions , respectively.

Figure 15 shows the effect of decreasing the initial out-of-straightness to L/10,000 (dashed curves) which is close to the average measured value for five identical lengths reported in *Section 2.1*. The effect is similar to that discussed above for the weak axis. Even though the out-of-straightness might generally be much smaller for the strong axis, it is likely that the L/1000 value will continue to be assumed in design developments as it has for the past 100 years.
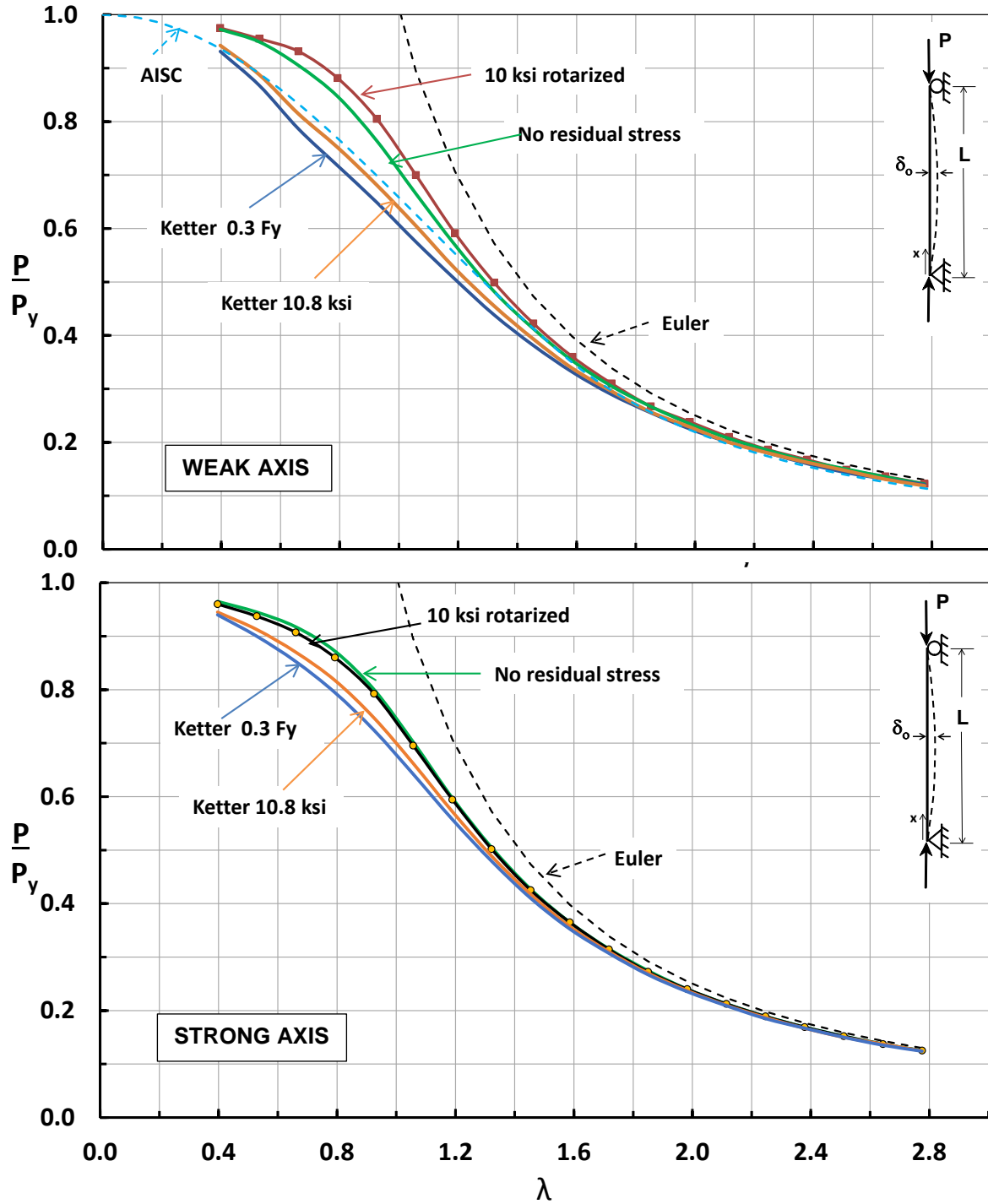
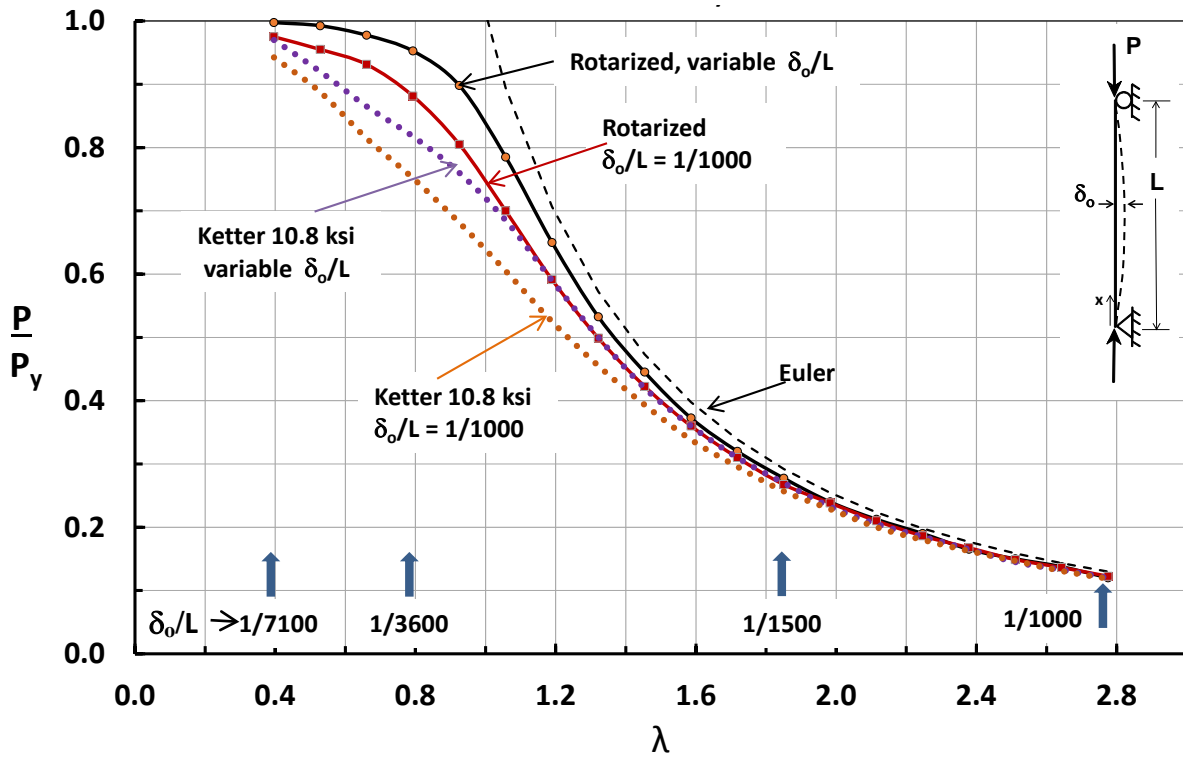Figure 13: Effect of Residual Stresses - Sine $\delta_o = L/1000$

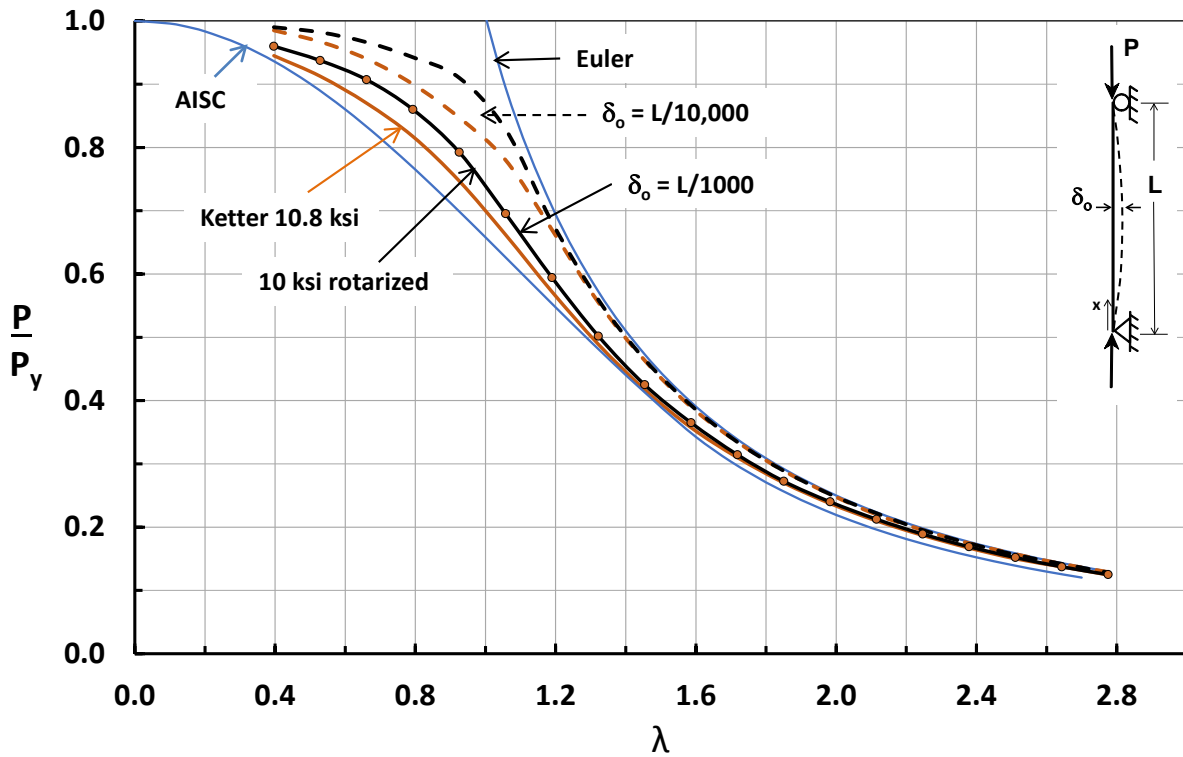Figure 14: Weak Axis W12x65: Effect of Variable δ_o / L

Figure 15: Strong Axis W12x65: Effect of δ_o / L

5. Proposed Design Recommendation

For design of columns that are rotary straightened, it is proposed that the column curve(s) be conservatively based on the ultimate strength of a member with $\delta_o /L = 1000$ and no residual stresses. Those column curves are shown by the solid black and red lines in Fig. 16 for strong and weak axis strength and based on a FEM 2nd order inelastic analysis program, ABAQUS, that is not practical for typical design. The two curves are very close to each other and a single curve could be fit to represent this ultimate strength for design. However, the following interaction equation was found to give excellent predictions of the ultimate column strength:

$$\frac{P}{P_y} + \frac{M_{2nd\,order\,elastic}}{M_p} = 1 \tag{1}$$

where $M_{2nd\,order\,elastic}$ is based on an initial moment, M = .001 L×P, and M_p is the plastic moment about the particular bending axis. The dashed lines in Fig. 16 have been generated directly by Eq. 1. In the case of an axially loaded column with a sine curve initial imperfection, the exact $M_{2nd\,order\,elastic\,moment} = 0.001PL \div (1- P/P_e)$, the amplified first order moment, where P_e is the Euler load. Eq. 1 is just a modified version of the classic Aryton-Perry (1886) formula for the exact first yield capacity of a column with an initial out-of-straightness where M_y, the moment capacity at first yield, has been replaced by M_p. On average Eq. 1 gives results within 1.7% of the ABAQUS solution with a maximum difference of 3.1% for the weak axis and within an average of 1.4% with a maximum difference also 3.1% for the strong axis.
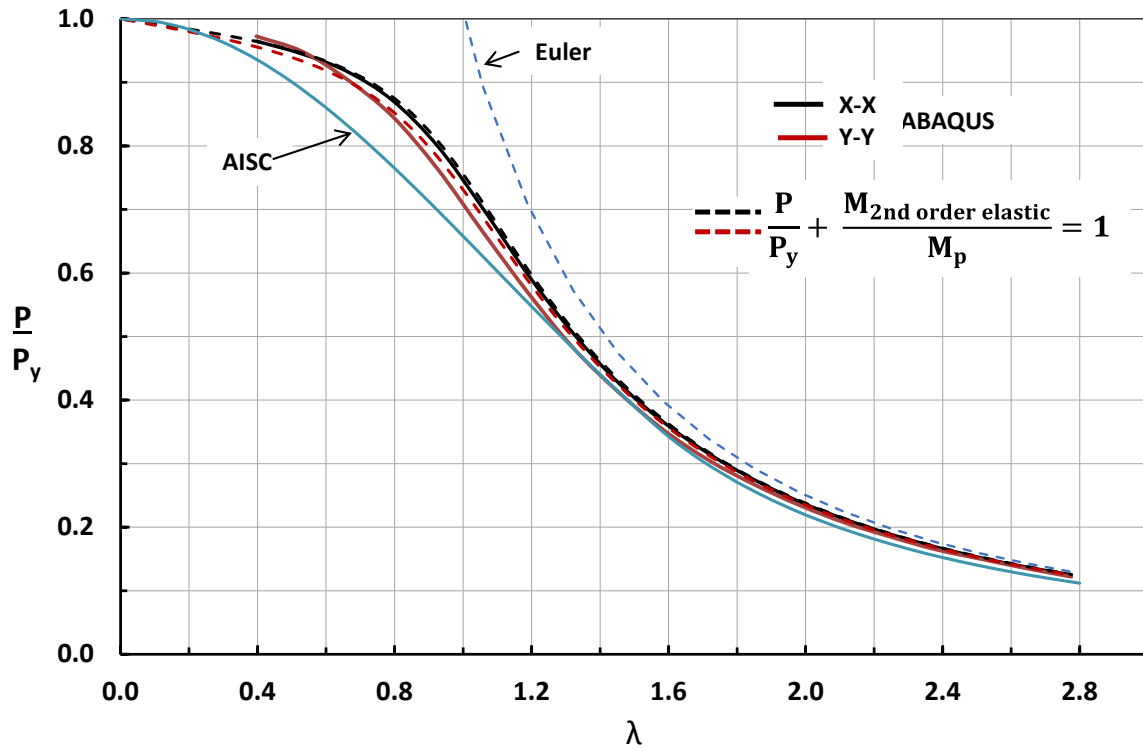

Figure 16: Column Design Interaction Equation

14

A pilot study to investigate the effect of rotarizing on the behavior of columns in frames and beam-columns was conducted on the structures shown in center of Fig. 17. Actually only the beam-column with a concentrated lateral load at midspan was analyzed because the pinned-end frame with half the length of the beam-column is mathematically the same problem. In all four plots the W12x65 column had a L/r = 80. Strong and weak axis bending were evaluated at two different axial load levels, $P/P_y = 0.4$ and 0.5. Within each plot of lateral load H vs deflection Δ three residual stress case were analyzed, rotary-straightened with 10 ksi tension at the flange tips, no residual stress and the Ketter pattern with 0.3 Fy = 15 ksi for Fy = 50 ksi. This Ketter value was chosen so results could be checked against previous studies with 36 ksi material.

The beam-column was not loaded proportionally. The axial load was applied first to the column with initial $\delta_o/L = 1/1000$ causing additional lateral displacement because of the eccentricity. The displacement shown in the plots is not the total displacement at midspan but only the deflection occurring during the application of the lateral load. Displacement control was used to obtain data after the peak load was reached. It is clear from the plots that residual stresses have a much greater effect than was noted in the column curve study. For strong axis bending the behavior is elastic almost to the maximum load level for the rotarized and no residual stress cases. For weak axis bending the structural response is much different, mainly due to the almost 1.5 shape factor in the weak direction of W shapes. Significant plasticity must occur as the plastic moment is approached resulting in loss of stiffness and increased second order effects. Weak axis bending performance controls the development of general design approaches for beam-columns.

 The greatly improved performance of rotary-straightened beam-columns shows the relatively simple Eq. 1 appears to be a viable approach for designing beam-columns. In all four plots in Fig.17 the maximum load reached for the no residual stress case is noted along with the estimated strength derived from Eq.1, which was developed for the no residual stress case. For the two strong-axis cases the difference between the maximum load and results from Eq. 1 are less than 3 %. Even though Eq. 1 gives 7.3% unconservative difference, the effect of that difference only affects the interaction equation sum of two terms by 2.8%.

Aside from the economic advantages that Eq.1 provides for columns with L/r < 100, the fact that the axially-loaded column solution is mechanics based rather than a curve fit will improve the quest for direct computer evaluation of structural designs. For simple structures relatively easy hand methods that build on the B1 and B2 concepts in the AISC Specification can still be used because the case is being made for design based on 2nd order elastic analysis, not inelastic analysis. Also with P_y in the first term instead of P_{cr} based on story height as required in the current Direct Analysis AISC approach, similar problems such as the two in Fig. 17 will have the same solution.

Numerous issues must be resolved such as how to handle problems of members with compressive residual stresses at the flange tips as in welded built-up sections and large rolled sections that are gag straightened. This research can only be considered preliminary, but promising.
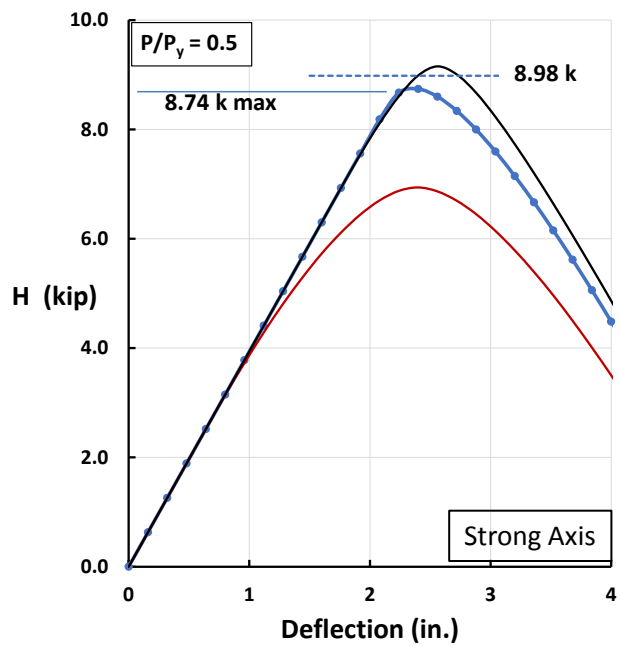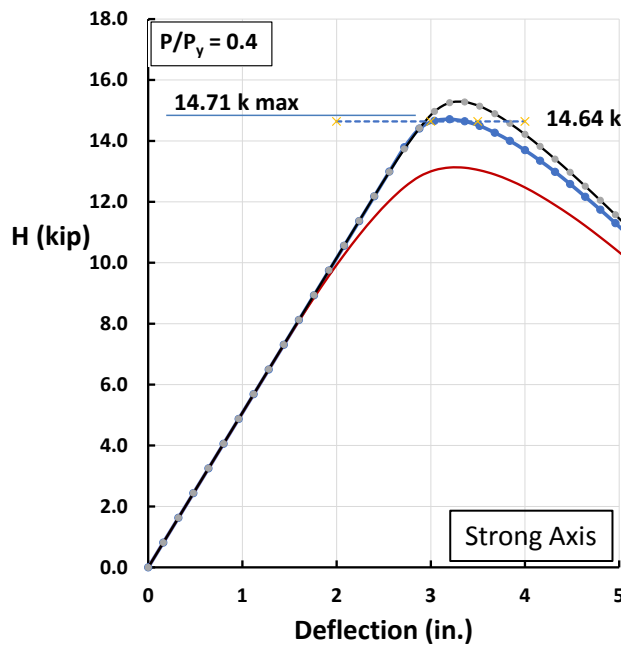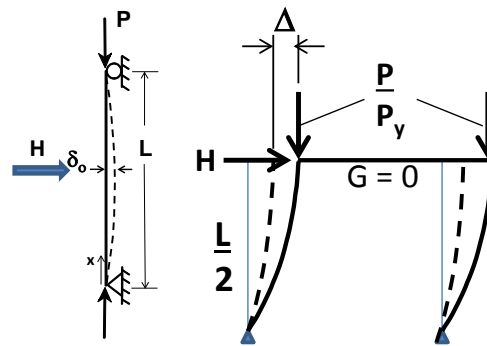
15
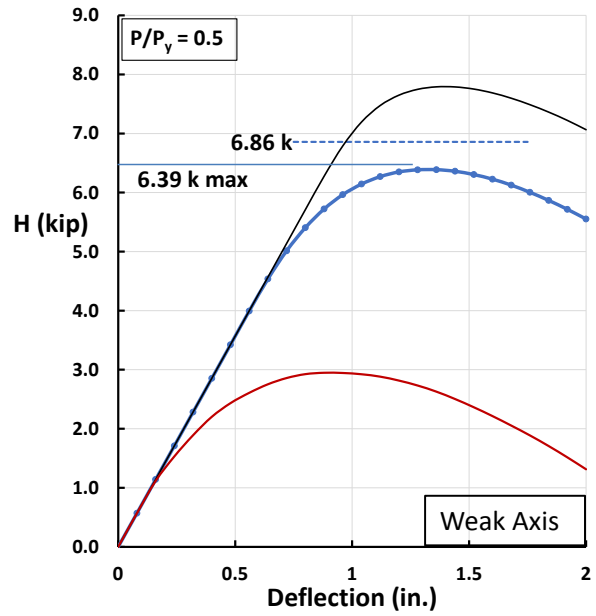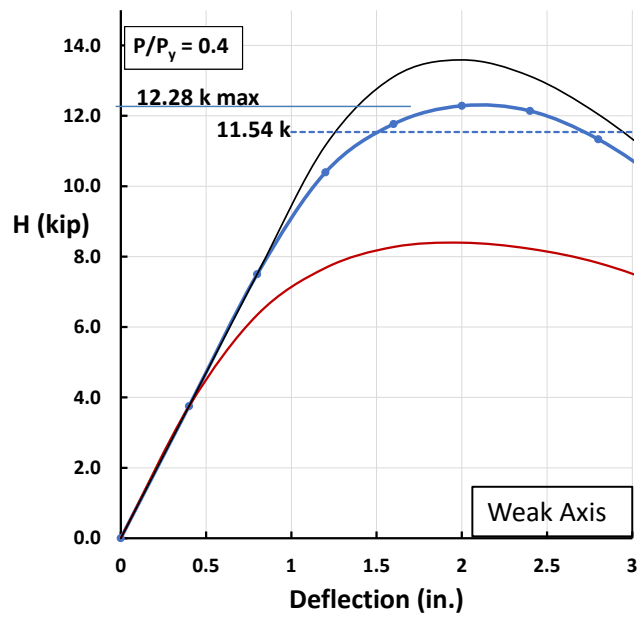
Figure 17: Laterally Loaded Beam-Column with L/r = 80 – Effect of Residual Stresses

6. Conclusions

It has been shown by some limited experiments that current rotary-straightening methods of most rolled sections eliminate the harmful compressive residual stresses at the flange tips. Column curves developed for such sections showed significantly improved strength for members with L/r < 100. The difference in column strength between the strong and weak axis is almost eliminated by rotarizing. A simple interaction formula, Eq. 1, was shown to predict the column capacity almost exactly. The interaction formula also gave good results in predicting the capacity of a very limited number of beam-column problems. Because this was a very limited study, no design recommendations are made.

Additional research is needed to obtain a broad spectrum of rotarized residual stress data and additional frame problems will need to be solved. Out-of-straightness data on currently produced sections that are rotary-straightened is sparse so such data would be useful in determining the realistic reliability of steel columns.

References

Alpsten, G. (1972). "Residual stresses, yield stress and column strength of hot-rolled and roller-straightened steel shapes." *Proceedings*, First International Colloquium on Stability, Paris, 38-59. Published by IABSE in 1975.

ASTM. (2015). A992/A992M-11 Standard Specification for Structural Steel Shapes.

ASTM. (2016). Standard Methods for Tension Testing of Metallic Materials.

Aryton, W, Perry, J. (1886). "On struts." *The Engineer*, London, 62 (12) 464, 513.

Beedle, L.S., Tall, L. (1960). "Basic column Strength." *Journal of the Structural Division*, ASCE, 86 (ST7)139-173.

European Convention for Constructional Steelwork (ECCS), (1976). "Cold-straightened compression members." Manual on the Stability of Compression Members, Introductory Report, 2nd International Colloquium on Stability, Section 3.1.4, 91-97.

Galambos, T. V. (1983). "Reliability of axially loaded columns." *Engineering Structures*, 5(1), 73-78.

Gozum, A. T., & Huber, A. W. (1955). Material properties, residual stresses and column strength. *Lehigh University*.

Ketter, R.L., Kaminsky, F.L., Beedle, L.S. (1955). "Plastic deformation of wide-flange beam-columns." *Transactions*, ASCE, 120, 1028-1061.

Shen, Z. Y., Lu, L. W. (1983). "Analysis of initially crooked, end restrained steel columns." *Journal of Constructional Steel Research*, 3(1), 10-18.

Simulia, D. (2017). Analysis User Manual. Abaqus/Standard.

Structural Stability Research Council (SSRC), (2010). *Guide to stability design criteria for metal structures*, Ziemian, R. ed, Wiley, Hoboken, NJ.

Tebedge, N., Alpsten, G., Tall, L. (1973). "Residual-stress measurement by the sectioning method." *Experimental Mechanics*, 13(2), 88-96.

Tebedge, N.,Tall, L. (1974). "Residual stresses in structural steel shapes: a summary of measured values." *Construction Metallique*, 2(1974) 37-48. English translation of text, *Fritz Laboratory Report 337.34*, Feb. 1973 (74-12) 20p.

Yang, B., Nie, S., Xiong, G., Hu, Y., Bai, J., Zhang, W., Dai, G. (2016). "Residual stresses in welded I-shaped sections fabricated from Q460GJ structural steel plates." *Journal of Constructional Steel Research*, 122, 2, 261-273

Yura, J.A., Lu, L.W. (1968). Ultimate load tests on braced multi-story frames. Fritz laboratory Report 272.60, 46p.

Yura, J.A. (2018). "Column design: past, present, future." *Proceedings of the Annual Stability Conference*, Structural Stability Research Council, 20p.